Modulation of the E-cadherin/β-catenin signaling pathway in human cells infected *in vitro* with *Coxiella burnetii*

Running title: E-cadherin pathway modulation during *Coxiella burnetii* infection

Ikram OMAR OSMAN[1,2], Soraya MEZOUAR[1,2], Djamal BELHAOUARI-BRAHIM[1,2], Jean-Louis MEGE[1,2], Christian Albert DEVAUX[1,2,3*].

[1]Aix-Marseille Univ, IRD, APHM, MEPHI, Marseille, France

[2]IHU-Méditerranée Infection, Marseille, France

[3]CNRS, Marseille, France

[*]Corresponding author:

Christian Devaux, PhD

Email: christian.devaux@mediterranee-infection.com

Abstract :

High concentration of soluble E-cadherin (E-cad) was previously found in sera from Q fever patients. Here, BeWo cells which express a high concentration of E-cad were used as an *in vitro* model to investigate the expression and function of E-cad in response to infection by *Coxiella burnetii*, the etiological agent of Q fever. Infection of BeWo cells with *C. burnetii* leads to a decrease in the number of BeWo cells expressing E-cad at their membrane. A shedding of soluble E-cad was associated with the post-infection decrease of membrane-bound E-cad. The modulation of E-cad expression requires bacterial viability and was not found with heat-inactivated *C. burnetii*. Moreover, the intracytoplasmic cell concentration of β-catenin (β-cat), a ligand of E-cad, was reduced after bacterial infection, suggesting that the bacterium induces modulation of the E-cad/β-cat signaling pathway and *CDH1* and *CTNNB1* genes transcription. Finally, several genes operating the canonical Wnt-Frizzled/β-cat pathway were overexpressed in cells infected with *C. burnetii*. This was particularly evident with the highly virulent strain of *C. burnetii,* Guiana. Our data demonstrate that infection of BeWo cells by live *C. burnetii* modulates the E-cad/β-cat signaling pathway.

50 **1. Introduction**

51 *Coxiella burnetii*, a known intracellular bacterium causing Query (Q) fever in humans, is
52 most often transmitted to humans through products derived from infected animals[1], and primarily
53 targets the lungs. The bacterium infects a large spectrum of susceptible cells, including myeloid
54 cells[2,3], trophoblasts[4] and adipocytes[5]. Human primary infection remains asymptomatic in
55 most people (around 60% of cases)[6]. In the other cases, symptoms develop within 2-6 weeks
56 after *C. burnetii* exposure and mainly consist of hepatitis, endocarditis, pneumonia, vascular
57 infection and lymphadenitis[7,8]. Although these symptoms usually resolve in a few weeks, in rare
58 cases (less than 5%), the infection become persistent and progresses to chronic endocarditis[9].
59 Factors that may determine the severity of the disease remain mostly unknown[10–13], but
60 considerable genomic heterogeneity was reported among *C. burnetii* strains[14–18], and gene
61 deletion was associated with a higher strain virulence[19]. A role for the bacterial
62 lipopolysaccharide (LPS) was also highlighted, since several *in vitro* passages of the virulent Nine
63 Mile strain of *C. burnetii* generate an avirulent strain characterized by a truncated LPS with the
64 absence of the terminal sugar-containing O-polysaccharide chain[19,20].

65 In the past decade, a diagnosis of Q fever with persistent focal infection was reported as an
66 increased risk factor for B-cell lymphoma [21–23]. Overproduction of interleukin (IL)-10, a B-cell
67 growth factor[24], is critical for sustaining *C. burnetii* replication[25], and might possibly favor
68 lymphoma occurrence [22]. In peripheral blood mononuclear cells (PBMCs) of Q fever patients it
69 was possible to characterize a transcriptional signature (overexpression of genes involved in the
70 anti-apoptotic process or repression of pro-apoptotic pathways), that could be, in very rare cases,
71 associated with the development of non-Hodgkin lymphoma (NHL)[26]. We also speculated that
72 if *C. burnetii* infection could sometimes promote the development of NHL, the early steps towards

73 NHL progression might be the decrease of E-cadherin (E-cad) surface expression on the $CD20^+$ B-
74 cells subpopulation of PBMCs (E-cad positive B-cells represents less than 1% of the circulating B
75 lymphocytes) from *C. burnetii*-infected patients [27]. However, until now the molecular
76 mechanisms that could account for the progression of the disease to lymphoma have remained
77 elusive. Moreover, these results are controversial, and other studies of Q fever patients have not
78 confirmed the link between Q fever and NHL[28]. A recent large analysis of the Dutch population
79 incorporating the 2007-2010 Q fever outbreak (266 million people including 61424 diagnosed with
80 NHL and 4310 persons diagnosed with acute Q fever), concluded to the lack of increased risk of
81 NHL after Q fever[29].

82 We previously found that sE-cad is present in higher concentrations in sera of Q fever
83 patients than healthy controls[27], and postulated that E-cad cleavage may be a step towards *C.*
84 *burnetii*-invasion of the host during Q fever. Increasing evidence can be found in the literature
85 indicating that cadherins may play a major role during the development of infectious diseases[30].
86 Among cadherins, the E-cadherin (E-cad), a 120 kDa adhesion cell-surface protein, is known for
87 its role in cell-to-cell tight junctions ensuring integrity of epithelial barriers. E-cad also behaves as
88 a signaling molecule through its intra-cytoplasmic tail that binds second messengers, thereby
89 having roles in cell activation, cell division, and cell differentiation and/or invasion[31,32]. Besides
90 its role in inter-cellular adhesion, E-cad behaves as a tumor suppressor[33–35] and plays a major
91 role in cancer invasion/metastasis[36–38]. Cell reprogramming can be achieved by the release of
92 sE-cad generated from the cleavage of the extracellular domain of E-cad[39]. E-cad is known to be
93 a target for several bacterial sheddases, leading to the release of sE-cad[39,40].

94 Here we developed an *in vitro* cellular model with BeWo cells which express a high
95 concentration of E-cad at their surface[41] and are susceptible to *C. burnetii* infection[4] to study
96 the effect of *C. burnetii* infection on the expression of E-cad and evidenced that *C. burnetii*

97 infection modulates expression of the E-cad/β-catenin signaling pathway by acting on *CDH1* and
98 *CTNNB1* gene transcription, on cell-surface expression of E-cad, the release of sE-cad and the
99 cytosolic pool of β-catenin.
100

101 ## 2.Materials and Methods

102 ### 2.1.*Coxiella burnetii*

103 *Coxiella burnetii* (Nine Mile strain RSA496, Guiana Strain Cb175) was grown as described[42].
104 L929 cells line were used for *in vitro* culture using a Minimum Eagle medium (MEM, Invitrogen,
105 USA) supplemented with 4% fetal bovine serum (FBS, Invitrogen, USA) and 1% 2mM L-
106 glutamine (Invitrogen, USA) and then incubated at 35°C in a 5% CO_2 atmosphere. After three
107 passages infected cells were sonicated, and the cell-free supernatants were centrifuged to harvest
108 the bacteria, which were then washed and stored at -80°C until use. Gimenez staining and qPCR
109 (using the *com-1* gene) were used to determine the concentration of bacteria in the sample.
110

111 ### 2.2. *In vitro* cell culture model

112 Blood samples (leucopacks) used in our study come from the French Blood Establishment
113 (Etablissement français du sang, EFS), which carries out donor inclusions, informed consent and
114 sample collection. Through a convention established between our laboratory and the EFS
115 (No.7828), buffy coats were obtained from healthy blood donors. Peripheral blood mononuclear
116 cells (PBMCs) were isolated after centrifugation on Ficoll cushions (MSL, Eurobio, France).
117 Monocytes (5-15% of the total number of PBMCs) were obtained from PBMCs using magnetic
118 beads coated with monoclonal Abs directed against CD14, according to the manufacturer's
119 instructions (Miltenyi Biotech, France). Monocytes-derived-macrophages (MDM) were obtained

120 following the incubation of monocytes with 10% heat-inactivated human AB serum (MP
121 Biomedicals, LLC, France) during a 3-day culture followed by 4 days of incubation with 10% FBS
122 (Invitrogen, USA) as previously described[43]. Monocyte-derived- dendritic cells (moDC) were
123 obtained by incubation of monocytes with 1 ng/mL of granulocytes-macrophages colony-
124 stimulating factor (GM-CSF, R&D Systems, France) and Interleukin-4 (R&D Systems, USA) for
125 7 days as previously described[44]. Mast cells were obtained from PBMCs as previously
126 described[45]. All cells were cultured in Roswell Park memorial institute (RPMI) 1640 medium
127 (Gibco, Thermo Fisher, USA) supplemented with 10% FBS.
128 The human trophoblastic BeWo cell line was purchased from the American type culture collection
129 (ATCC, CCL-98, Bethesda, USA) and cultured in a Dulbecco's Modified Eagle Medium F-12
130 Nutrient Mixture (DMEM F-12, Invitrogen, USA) containing 10% FBS. The HeLa cell line (ATCC
131 CCL-2), a human epithelial cell line derived from a cervical cancer, was cultured in DMEM
132 supplemented with 10% FBS and 1% L-glutamine (Invitrogen, USA). MRC-5 (ATCC CCL-171),
133 a human embryonic fibroblast cell line obtained from an aborted fetus, was cultured in MEM
134 supplemented with 4% FBS and 1% L-glutamine. THP-1 (ATCC TIB-202), a human monocytic
135 cell line derived from an acute monocytic leukemia patient, was maintained in RPMI 1640 medium
136 supplemented with 10% FBS and 1% penicillin/streptomycin (Gibco) at 37°C and 5% CO_2.
137

138 **2.3. Microarray and data analysis**

139 The microarray was performed as previously described[26] with data submitted to NCBI's Gene
140 Expression Omnibus (GEO series accession number GSE112086). Briefly, RNAs were extracted
141 using an RNeasy Mini Kit (QIAGEN SA, France) with a DNase I step, then labeled using Cyanin-
142 3 CTP (Agilent Technologies) and hybridized on chips containing 45000 probes (4x44K Whole
143 Human Genome). After hybridization, slides were washed and scanned with a pixel size of 5 µm

144 using the DNA Microarray scanner G2505C. The raw data were extracted (Extraction Software
145 10.5.1) and processed using GeneSpring GX 14.9 software (Agilent Technologies). A selection
146 filter of both statistical value $p<0.01$ (t-Student test) and an absolute value of fold change (FC)
147 greater than 1.5 was used to identify differentially expressed genes. Modulated genes were
148 analyzed using ClustVis software.
149

150 **2.4. Quantitative-Reverse Transcription Polymerase Chain Reaction (qRT-PCR)**

151 BeWo cells ($2x10^5$ cells/well) were cultured in flat-bottom 24-well plates for 12 h and were then
152 infected with the live virulent *C. burnetii* Nine Mile (NMI) and Guiana (GuiI) strains or were
153 exposed to heat-inactivated virulent *C. burnetii* NMI strains at a 100:1 bacterium-to-cell ratio, or
154 stimulated with 100 ng/mL of lipopolysaccharide (LPS) from *E. Coli* (O55:B5; Sigma-Aldrich,
155 USA) for 48 h at 37°C in a 5% CO_2 atmosphere. RNAs were extracted as described above. The
156 first-strand cDNA was obtained using oligo(dT) primers and Moloney murine leukemia virus-
157 reverse transcriptase (MMLV-RT kit; Life Technologies, USA), using 100 ng of purified RNA.
158 The qPCR experiments were performed using specific oligonucleotide primers and hot-start
159 polymerase (SYBR Green Fast Master Mix; Roche Diagnostics, Germany). The amplification
160 cycles were performed using a C1000 Touch Thermal cycler (Biorad, USA). Specific primers used
161 in this study are listed in **Table 1** and the results were normalized using the housekeeping gene β-
162 actin (*ACTB*) (Fwd: 5' CAT GCC ATC CTG CGT CTG GA 3'; Rev: 5' CCG TGG CCA TCT CTT
163 GCT CG 3') and expressed as the relative expression ($2^{-\Delta CT}$) where $\Delta Ct = Ct_{Target} - Ct_{Actin}$, and as
164 the fold change ($2^{-\Delta\Delta CT}$), where $\Delta\Delta Ct = \Delta Ct_{stimulated} - \Delta Ct_{unstimulated}$ as previously described[46]. Ct
165 values were defined as the number of cycles for which fluorescence signals were detected.
166
167

168 **2.5. E-cadherin protein quantification**

169 BeWo cells ($5x10^5$ cells/well) were cultured in flat-bottom 12-well plates for 12 h and were then
170 infected with live *C. burnetii* NMI strains or exposed to heat-inactivated *C. burnetii* strains at a
171 50:1 bacterium-to-cell ratio or stimulated with 100 ng/mL of LPS for 4, 24 and 48 h at 37°C in a
172 5% CO_2 atmosphere.

173 For each kinetics, the culture supernatants were collected, centrifuged at 1000 g for 10 min and
174 stored at -20°C until use. The quantity of sE-cad in the supernatants was determined using a specific
175 immunoassay (DCADEO, R&D Systems, USA) according to the manufacture's instructions. The
176 minimal detectable concentration of human sE-cad was 0.313 ng/mL.

177 Protein quantification was evaluated using a western blot assay. Cells were washed with ice cold
178 phosphate buffered saline (PBS 1X) and lysed using 1X RIPA buffer (100 mM Tris-HCl pH 7.5,
179 750 mM NaCl, 5 mM EDTA, 5% IGEPAL, 0.5% sodium dodecyl sulfate (SDS), and 2.5% Na
180 deoxycholate) supplemented with both a protease and phosphatase cocktail inhibitor (Roche,
181 Germany). Ten µg of protein were loaded onto 10% SDS polyacrylamide gels. After transfer into
182 a nitrocellulose membrane, the blots were incubated overnight at 4°C with a saturation solution
183 (5% fat free milk (FFM)-1X PBS - 0.3% Tween 20). Blots were then incubated with mouse anti-
184 human E-cad ectodomain mAb (1:5000) (HECD-131700, Invitrogen, USA) for 2 h, followed by
185 an incubation with mouse anti-human E-cad cytoplasmic domain mAb (4A2C7, Life
186 Technologies). In some experiments, β-catenin was detected using an anti-human β-catenin
187 antibody (1:1000) (Agilent Dako, USA). After three washes in 1X PBS – 0.3% Tween 20, the blots
188 were incubated with horseradish peroxidase-conjugated sheep anti-mouse IgG (1:10000) for 2 h at
189 room temperature. β-actin expression was measured using an anti-human β-actin horseradish
190 peroxidase-conjugated mAb (1:25000, Life Technologies, USA) as the loading control. The
191 proteins were revealed using an ECL western blotting substrate (Promega, USA) and images were

192 digitized using a Fusion FX (Vilber Lourmat, France). The density of the bands was measured
193 using Image J v 1.8.0.
194
195 **2.6. Confocal immunofluorescence assay**
196 BeWo cells were cultured on sterile coverslips in 24-well plates at an initial concentration of 2×10^5
197 cells/well and were then infected with live virulent *C. burnetii* NMI strains or exposed to heat-
198 inactivated virulent *C. burnetii* NMI strain at a 50:1 bacterium-to-cell ratio or stimulated with 100
199 ng/mL LPS for 24 h at 37°C in a 5% CO_2 atmosphere. After fixation with 4% paraformaldehyde,
200 cells were permeabilized with 0.1% Triton X-100 for 3 min and saturated with 3% BSA – 0.1%
201 Tween 20 - PBS for 30 min at room temperature. Fixed cells were first incubated with a mouse
202 anti-E-cad cytoplasmic domain mAb (1:1000) (4A2C7, Life Technologies, USA) for 1 h at room
203 temperature and then with 1:500 rabbit polyclonal anti-*C. burnetii* antiserum. After washing, cells
204 were incubated for 30 min at room temperature with a mix (1:1000) of goat anti-rabbit IgG
205 secondary antibody (Alexa Fluor 647, Life Technologies, USA) and goat anti-mouse IgG
206 secondary antibody (Alexa Fluor-555, Life Technologies, USA). 4',6'-diamino-2-fenil-indol
207 (1:25000) (DAPI, Life Technologies, USA) and Phalloidin (1:500) (Alexa-488, OZYME, France)
208 were used for staining the nucleus and the filamentous actin, respectively. Labelled cells were
209 analyzed using laser scanning confocal microscopy and pictures were acquired using a confocal
210 microscope (Zeiss LSM 800) with a 63X/1.4 oil objective, an electronic magnification of 0.7 and
211 a resolution of 1014_1014 pixels.
212
213 **2.7. Flow cytometry assay**
214 BeWo cells (1×10^6 cells/well) were cultured in flat-bottom 6-well plates and were then infected
215 with a live virulent *C. burnetii* NMI strain at a 50:1 bacterium-to-cell ratio or stimulated with 100

216 ng/mL LPS for 24, 48 and 72 h at 37°C in a 5% CO_2 atmosphere. Cells were incubated with 2 mM
217 EDTA in PBS for 15 min at 4°C to release the adherent cells from the culture plate. After
218 centrifugation at 500 g for 5 min, the pellet was suspended in a FACS buffer (2 mM EDTA, 10%
219 FBS in PBS) and then incubated for 30 min with a mouse anti-human E-cad ectodomain antibody
220 (HECD-131700, 1:1000). After two washes, cells were incubated with a goat anti-mouse IgG Alexa
221 Fluor-555 secondary antibody. Fluorescence intensity was measured using a Canto II
222 cytofluorometer (Becton Dickinson/Biosciences, France) and the results were analyzed using
223 FlowJo V10.7.2 software (Becton Dickinson, USA).
224

225 **2.8. Electron microscopy analysis**

226 BeWo cells (1×10^6 cells/well) were cultured in flat-bottom 6-well plates and were then infected
227 with live virulent *C. burnetii* NMI and GuiI strains at a 100:1 bacterium-to-cell ratio at 37°C in a
228 5% CO_2 atmosphere. After 24 h of infection, the cells were fixed with 2.5% glutaraldehyde in 0.1
229 M cacodylate buffer for five hours at 4°C. Resin embedding was microwave-assisted with a
230 Biowave Pro+ (Pelco, Fresno, CA, USA). After washing twice with a mixture of 0.2-M
231 saccharose/0.1-M sodium cacodylate and once with distilled water, samples were progressively
232 dehydrated by successive baths in 50%, 70% and 96% ethanol. Substitution with LR–White resin
233 (medium grade; Polysciences, Warrington, PA, USA) was achieved by incubations with 25% to
234 100% LR–White resin and samples were placed in a polymerization chamber for 72 h at 60°C. All
235 solutions used above were 0.2-µm filtered. After curing, the resin blocks were manually trimmed
236 with a razor blade and dish bottoms were detached from cell monolayers by cold shock via
237 immersion in liquid nitrogen for 20 seconds. Resin blocks were placed in a UC7 ultramicrotome
238 (Leica), trimmed to pyramids, and ultrathin 100 nm sections were cut and placed on HR25 300
239 Mesh Copper/Rhodium grids (TAAB, Aldermaston, England). Sections were contrasted with

240 uranyl acetate and lead citrate. Grids were attached with double sided tape to a glass slide and
241 platinum-coated at 10 mA for 20 seconds with a MC1000 sputter coater (Hitachi High-
242 Technologies, Japan). Electron micrographs were obtained on a SU5000 SEM (Hitachi High-
243 Technologies, Japan) operated in high-vacuum at 10 kV accelerating voltage and observation mode
244 (spot size 30) with BSE detector.
245

246 **2.9. Statistical analysis**

247 The statistical analyses of the data were performed using GraphPad-Prism software (version 6.0).
248 The results are presented as the ± standard error of the mean (SEM). The Mann-Whitney U test
249 was used for flow cytometry, the two-way ANOVA test for E-cadherin quantification and
250 transcriptional analysis, and a nonparametric Kruskal-Wallis with Dunn's multiple comparison test
251 for group comparison. A p value <0.05 was considered statistically significant.
252

253 ## 3. Results

254 **3.1. Selection of the BeWo cell line as an appropriate cellular model to study E-cad expression**
255 **in cells infected with *C. burnetii***

256 It was previously reported that many cell types, including myeloid cells[47,48], trophoblasts[4,49],
257 lung cells[50,51], and adipocytes[5] are susceptible to *C. burnetii* infection. To conduct our study,
258 it was first necessary to select a cellular model with high expression of E-cad. To this end, we
259 evaluated E-cad expression in different cell lines, including HeLa (human cervical cancer cell line),
260 THP-1 (human monocytic cell line), MRC-5 (human fetal lung fibroblasts), BeWo (human placenta
261 choriocarcinoma cell line), and primary monocytes from healthy donors. As shown in **Fig 1A**,
262 using a western blot assay, BeWo cells were found to express the highest concentration of E-cad

263 and HeLa cells ranked second. Additionally, we also confirmed the highest membrane expression
264 of E-cad on BeWo cells by confocal microscopy (**Fig 1B**). This finding was consistent with the
265 reports from the literature on the common use of BeWo cells as a model to study E-cad
266 expression[52,53]. Moreover, scanning electron microscopy of *C. burnetii*-infected BeWo cells
267 (**Fig 1C** and **S1 Fig**) showed the presence of several vacuoles, either empty or containing electron-
268 dense circular structures, with diameters ranging from 250 nm to 700 nm dispersed in the cell
269 cytoplasm, corresponding to the morphology and size of *C. burnetii* as previously described[54].
270 Therefore, the BeWo cell line was chosen for further investigation because it has both sensitivity
271 to *C. burnetii* infection and high expression of E-cad.
272
273 **3.2. *C. burnetii* infection modulates cell surface expression of E-cad**
274 The level of E-cad protein expression at the cell surface of BeWo cells infected or not by *C. burnetii*
275 NMI was evaluated by flow cytometry, targeting the ectodomain portion of E-cad. Twenty-four
276 hours post-*C. burnetii* infection, the percentage of BeWo cells expressing membrane-bound E-cad
277 decreased significantly compared to LPS stimulated- and unstimulated- cells ($p<0.05$ and $p<0.01$,
278 respectively) used as controls (**Fig 2A and 2B**). Also, we found a significant decrease in the mean
279 intensity fluorescence signal of the E-cad in BeWo cells infected with *C. burnetii* compared to
280 LPS-stimulated and unstimulated cells ($p<0.05$ and $p<0.01$, respectively) (**Fig 2C**). Then, we
281 studied whether bacterial antigen/cell contact was sufficient to trigger E-cad modulation, or
282 whether infection was absolutely required to observe a change in E-cad expression. Thus, we
283 investigated by confocal microscopy E-cad expression on BeWo cells after 4 hours and 24 hours
284 of infection with live *C. burnetii,* while controls consisted of exposure to heat-inactivated bacteria
285 or LPS. Although for unstimulated BeWo cells a high level of fluorescence and homogeneity of E-
286 cad distribution was observed, this result was not limited to this experimental condition. The same

287 expression profiles were observed for BeWo cells after *E. coli* LPS stimulation or heat-inactivated
288 *C. burnetii* bacterium stimulation (**Fig 2D**). Interestingly, live *C. burnetii*-infected BeWo cells
289 presented a significant decrease of E-cad expression and also a short intracellular colocalization of
290 the E-cad fluorescence signal with the fluorescence signal associated with *C. burnetii* at early stage
291 of infection (**S2 Fig**). In contrast, a low E-cad fluorescence signal was observed in infection (live
292 *C. burnetii*-infected BeWo cells). This decrease of E-cad cell-surface expression was accompanied
293 by an actin rearrangement over time (as shown at 24 hours) which was faster when the cells where
294 infected with the virulent Guiana strain (**S3 Fig**). These results indicate that membrane-bound E-
295 cad expression is highly modulated during active *C. burnetii* infection of BeWo cells, while *C.*
296 *burnetii* bacterial antigens are not sufficient to trigger a massive E-cad modulation.
297

298 **3.3. Release of sE-cad by *C. burnetii*-infected BeWo cells and modulation of *CDH1*/E-cad and**
299 ***CTNNB1*/β-catenin gene transcription**

300 Since we previously reported that Q fever patients have high expression of serum sE-cad[27], we
301 aimed at investigating whether the decreased expression of membrane-bound E-cad in *C. burnetii*-
302 infected BeWo cells could be associated with a release of sE-cad after E-cad proteolysis. As shown
303 in **Fig 3A**, we measured progressive basal accumulation of sE-cad in the cell culture medium over
304 time (at 24 hours and 48 hours). Interestingly, sE-cad release was significantly higher ($p < 0.001$)
305 over time in infection conditions compared to control conditions (unstimulated and LPS-stimulated
306 BeWo cells). A further immunoblot detection of the products synthesized in *C. burnetii*-infected
307 cells evidenced two components: the integral 120 kDa E-cad, and a protein of about 60 kDa, a
308 proteolytic product of E-cad (**Fig 3C**). In contrast, only the 120 kDa E-cad was found in the control
309 experiments. It is worth noting that the expression of β-catenin, an intracellular ligand of E-cad,
310 was strongly decreased in BeWo cells under live *C. burnetii*-infection conditions. This was further

311 confirmed using a densitometry scanning of the band that showed a significant ($p<0.05$) decrease
312 of β-catenin in *C. burnetii*-infected BeWo cells.
313 In accord with the literature regarding the E-cad/β-catenin signaling pathway, our results suggest
314 a translocation of β-catenin into the cell nucleus, associated with a modulation of *CDH1*/E-cad
315 gene expression. To confirm this hypothesis, the expression of *CDH1*/E-cad and *CTNNB1*/β-
316 catenin gene transcription was analyzed by qRT-PCR. Both *CDH1* and *CTNNB1* genes were found
317 significantly overexpressed ($p<0.01$ and $p<0.05$, respectively) in BeWo cells with *C. burnetii*
318 infection compared to cells exposed to *E. coli*-LPS (**Fig 3B**). These results indicate that *C. burnetii*
319 infection of BeWo cells induces a shedding of the E-cad protein ectodomain at an early stage of
320 the infection (detectable at 24 hours post-infection) and suggest that sE-cad shedding is associated
321 with the nuclear translocation of β-catenin and subsequent up-regulation of *CDH1* and *CTNNB1*
322 gene transcription through a feedback control loop.
323

324 **3.4. *C. burnetii* modulates expression of genes from both the E-cad/β-catenin pathway and**
325 **the Wnt/frizzled/β-catenin pathway in BeWo cells.**

326 To further demonstrate that the overexpression of *CDH1* and *CTNNB1* genes found in *C. burnetii*
327 infection of BeWo cells is not strain-dependent, BeWo cells were exposed for 48 hours to either
328 the live Nine Mile strain of *C. burnetii* or the more virulent Guiana (Cb175) laboratory strains of
329 *C. burnetii.* Heat-inactivated *C. burnetii* (Nine Mile strain) and *E. coli* LPS were used as controls.
330 As shown in **Fig 4A and 4B,** a significant overexpression of *CDH1* and *CTNNB1* genes was found
331 in BeWo cells infected with each of the two live strains of *C. burnetii*, extending our earlier
332 observations, illustrated in **Fig 3C**. In contrast, when BeWo cells were exposed to heat-inactivated
333 bacteria, *CTNNB1* gene expression was further increased and *CDH1* was significantly decreased.

334 These data suggest that the interaction of bacterial antigens with BeWo cells is sufficient to trigger
335 signals leading to *CTNNB1* gene transcription, while induction of *CDH1* requires infection.
336 We then explored the expression of several other genes known to encode proteins linked to the E-
337 cad/β-catenin and Wnt/frizzled/β-catenin axis, including *WNT3A*, *WNT5A*, *WNT9b*, *FZD1*, *APC*,
338 *NKD2*, *BCL9*, *TCF7L2* and *CNND1*. As shown in **Fig 4C**, most of these genes were overexpressed
339 in *C. burnetii*-infected BeWo cells, some of which (e.g., *BCL9*, *Wnt3A*) being also overexpressed
340 when BeWo cells were exposed to heat-inactivated-bacteria infected cells. Notably, *BCL9*, *WntA3*,
341 and *FDZ1* genes were significantly overexpressed where cells were infected with the live and more
342 virulent Guiana strain of *C. burnetii* compared to infection with the live Nine Mile strain. We also
343 observed that the gene coding for the tumor suppressor *APC* was significantly overexpressed after
344 BeWo cell exposure to *E. coli* LPS. It is worth noting that the *CCND1* gene coding for cyclin D1
345 kinase, a cell cycle activator and oncogenic protein, was significantly over-transcribed in cells
346 infected with live *C. burnetii*, notably in cells infected with the Nine Mile strain. The *CCND1* gene
347 is much less expressed with heat-inactivated bacteria, suggesting that activation of this gene
348 requires infection of cells by live bacteria. In addition, we also used a micro-array technology to
349 compare the expression of a set of 45000 genes in BeWo cells, infected or not by *C. burnetii*. This
350 approach indicated that 12189 genes were down-modulated after live *C. burnetii* infection of BeWo
351 cells, while 6492 genes were found up-regulated, among which genes such as *CDH1, CCND1, and*
352 *FZD1* were found highly expressed compared to their transcription levels in uninfected BeWo cells
353 (**S4 Fig**).
354 The transcriptomic results illustrated in Figure 4 were subjected to a principal component analysis
355 (PCA) and a hierarchical clustering heatmap was regenerated. This analysis highlighted distinct
356 gene expression profiles (**Fig 5**), the first one corresponding to live *C. burnetii* strain infectious
357 conditions, with slight differences between live *C. burnetii* strains, while other profiles

358 corresponded to unstimulated cells, LPS stimulated cells and cells exposed to heat-inactivated *C.*
359 *burnetii*. Genes activated by the live *C. burnetii* strain infection cluster together and show a
360 mirrored gene expression compared to other conditions. These results indicate that live *C. burnetii*
361 specifically induce *CDH1*, *CCND1, CTNNB1* and *BCL9* gene overexpression in BeWo cells.
362 However, for induction of the BCL9 gene, infection is not required, and transcription can be
363 stimulated by simply exposing the cells to *C. burnetii* bacterial antigens.
364

365 **4. Discussion**

366 We report here the first experimental evidence that differential gene expression analysis shows
367 modulation of the E-cadherin/β-catenin pathway signature during *C. burnetii* infection *in vitro* and
368 that this modulation results in disruption of E-cad expression on the cell surface. As a strictly
369 intracellular bacterium, and in order to establish a replication niche, *C. burnetii* forms intimate
370 interactions with its hosts, which aid in avoidance of the host immune response. In addition to the
371 immune response, *C. burnetii* must overcome another central host defense mechanism, apoptosis.
372 The molecular crosstalk between the bacterium and the host affects the induction of apoptosis,
373 thereby prolonging its survival.

374 We previously reported that activation of protein tyrosine kinases (PTK) by *C. burnetii* in
375 TPH-1 monocytes reflects *C. burnetii* virulence, since avirulent variants were unable to stimulate
376 PTK[55]. Additionally, modulation of cell signaling following *in vitro C. burnetii* infection of the
377 TPH-1 human macrophage-like cell line was also reported by Voth and Heinzen[56], who found
378 that infection directs the sustained activation of host pro-survival kinases Akt and Erk1/2, necessary
379 for anti-apoptotic activity that can conduct the development of certain lymphomas. Menelotte et
380 al.[22] were able to link the development of B-cell non-Hodgkin lymphoma to *C. burnetii* infection.
381 Despite intensive work to identify the bacterial compounds supporting *C. burnetii* replication and

382 virulence[11–13], the molecular mechanisms involved in *C. burnetii*-induced Q fever and possibly
383 associated NHL remain largely unknown. In more recent investigations[26] and working on Q
384 fever patient samples, we found that specific genes involved in anti-apoptotic processes (e.g., *BCL-*
385 *2*) were highly expressed, whereas pro-apoptotic genes were repressed in PBMCs from patients
386 with *C. burnetii*-associated NHL, supporting possible involvement of the corresponding proteins
387 in lymphomagenesis. However, these results remain controversial since other studies have not
388 confirmed the link between Q fever and NHL[28],[29].
389 The aim of the present study was to investigate *in vitro* the ability of *C. burnetii* to induce a
390 modulation of the E-cad/β-cat axis during infection. For this purpose, BeWo cells, which are
391 susceptible to *C. burnetii* infection, were used for their high expression of E-cad at the cell
392 membrane. As a result, we were able to demonstrate that the presence of *C. burnetii* in the cells
393 triggers overexpression of most of the genes of the signaling pathway, in particular *CDH1* genes
394 coding for the E-cad protein. Indeed, E-cad is known as a tumor suppressor trans-membrane protein
395 that inhibits β-cat activity by sequestrating it into the cell cytoplasm through interaction *via* the E-
396 cad cytoplasmic domain. In addition, cleavage of the E-cad protein by proteases (known as
397 sheddases) and excretion of a soluble fraction of E-cadherin (sE-cad) can contribute to cellular
398 transformation through the loss of cell-to-cell adhesion[57]. This is considered to be a triggering
399 event, promoting translocation of β-cat to the nucleus, where it forms complexes with BCL9 and
400 T-cell factor (TCF), leading to transactivation of cell cycle genes such as cyclin kinase *D1/CCND1*
401 and increased cell proliferation[58,59]. Moreover, the generation of sE-cad through sheddases and
402 the subsequent nuclear re-localization of β-cat may be a critical indicator for cancer development.
403 The induction of carcinogenic cascades via the E-cad/β-cat axis was reported in gastric
404 adenocarcinoma associated with *Helicobacter pylori* infection, in which the bacterium activates
405 calpain sheddase[60], or in myeloid-cell dependent distal colon tumorigenesis associated with

406 *Bacteroides fragilis* toxin, a known bacterial sheddase[61,62]. We recently reported[27] that E-cad
407 is cleaved in cells infected by *C. burnetii*. We demonstrated that, in addition to modulating *CDH1*
408 expression at the transcriptomic level, infection with *C. burnetii* leads to disruption of E-cad at the
409 cellular surface of BeWo cells. Under infection conditions, we observed a reduction of E-cad
410 expression at the cell surface that is likely due to cleavage of the extracellular fraction of the
411 protein, as its concentration in the supernatant is continuously increasing over time and the *CDH1*
412 gene is overexpressed. In BeWo cells infected with live *C. burnetii*, we observed a remodeling of
413 the actin filament, which triggers a morphological change. This particular effect was reported for
414 the first time in the study of Meconi et al.[63,55], in which they showed that virulent *C. burnetii*
415 stimulated morphological changes in human monocytes via the reorganization of the actin
416 cytoskeleton. As E-cad is linked to the actin cytoskeleton through β-cat and α-cat, a rearrangement
417 of the actin bundle can modify the adhesive function of E-cad and play an active role in the
418 migratory activity of carcinoma cells[64]. In the case of *C. burnetii* infection, the bacterium,
419 through the disruption of E-cad, may exploit the actin cytoskeleton to modulate its internalization
420 by host cells. An interesting observation that emerged from this study concerns the decreased
421 amount of β-cat protein in the cells, even though it is overexpressed at the transcriptomic level in
422 cells infected with the live bacterium. As β-cat is part of the canonical Wnt-Frizzled/ β-cat pathway,
423 we investigated most of the gene operating in the axis and as a result the expression of the genes
424 *WNT3A* (encoding the extracellular Wnt molecules that bind Frizzled/low-density lipoprotein-
425 receptor related proteins (LPR) complex and act on the canonical Wnt signaling pathway),
426 *FZD1*/Frizzled (Wnt receptor), *NKD2* (Wnt pathway regulator protein) were significantly
427 overexpressed in cells infected with live bacterium, mainly those infected with the more virulent
428 Guiana strain (Cb175). Interestingly, it has been shown that the activation of the Wnt/ Frizzled//β-
429 catenin pathway led to altered expression of genes involved in cell cycle regulation and apoptosis

430 in normal and leukemic B-cell progenitors[65]. In a previous publication, an overexpression of
431 transcription factor TCF7L2 and BCL9 was found, which is known to promote tumor progression
432 by conferring enhanced proliferation, metastatic, and angiogenic properties to cancer cells[66].
433 This may indicate that in the extremely rare cases of patients with *C. burnetii*-associated NHL, a
434 possible activation signal leads to lymphoma initiation. Furthermore, we also note that the
435 expression of the tumor suppressor adenomatous polyposis coli (APC) is repressed in infected cells
436 compared to the other conditions, suggesting that *C. burnetii* promotes the canonical Wnt signaling
437 pathway. Similar results were obtained from the microarray analysis of the Wnt/Frizzled/β-catenin
438 pathways in BeWo cells gene expression. Obviously, we are well aware of having used in this
439 study a particular cell model, a human trophoblastic cell line, and that under these conditions there
440 is a risk to overstate the biological significance of our data with the aim of explaining certain
441 aspects of the pathophysiology of Q fever. In fact, B cell analysis, which would have been more
442 physiologically relevant, was not possible because the CD20+E-Cad+ cells represent less than 1%
443 of circulating B cells, as we published in a previous article[27]. However, this BeWo model is very
444 useful for studying the link between infection by *C. burnetii* and modulation of the expression of
445 E-cad and provided a possible molecular basis for explaining the increase in sE-cad concentrations
446 in sera of Q fever patients [27].
447 In conclusion, this work provides for the first time evidence of the disruption of E-cad both at the
448 transcriptomic and cell surface levels by *C. burnetii*, opening a new avenue of research in
449 understanding the pathophysiology of Q fever. We hypothesize that the cleavage of E-cad by *C.*
450 *burnetii* could be a means to ensure its transmigration in order to modulate the reactivity of immune
451 cells and thus facilitate *C. burnetii* progression towards the target organs. Furthermore, the release
452 of sE-cad and overexpression of Wnt/Frizzled/β-catenin may participate in the molecular crosstalk
453 that occurs in the lymph node microenvironment during persistent Q fever and, in very rare cases,

454 triggering a pro-carcinogenic program. Finally, it can be hypothesized that the decrease in the
455 surface expression of E-cad induced by *C. burnetii* influences the replication of the bacterium or
456 its virulence.
457

458 **Acknowledgments**

459 We thank Prof. Jean Christophe LAGIER and Didier RAOULT for stimulating discussions and
460 unwavering support.
461
462
463
464
465
466
467
468
469
470
471
472
473
474
475
476
477

478 **References:**

479 1. Maurin M, Raoult D. Q fever. Clin Microbiol Rev. 1999;12:518-53.

480 2. Baca OG, Li Y-P, Kumar H. Survival of the Q fever agent Coxiella burnetii in the
481 phagolysosome. Trends in Microbiology. 1994;2:476-80.

482 3. Ghigo E, Pretat L, Desnues B, Capo C, Raoult D, Mege J-L. Intracellular Life of Coxiella
483 burnetii in Macrophages: An Update. Annals of the New York Academy of Sciences.
484 2009;1166:55-66.

485 4. Ben Amara A, Ghigo E, Le Priol Y, Lépolard C, Salcedo SP, Lemichez E, et al. Coxiella burnetii,
486 the Agent of Q Fever, Replicates within Trophoblasts and Induces a Unique Transcriptional
487 Response. PLoS One. 2010;5:e15315.

488 5. Bechah Y, Verneau J, Ben Amara A, Barry AO, Lépolard C, Achard V, et al. Persistence of
489 Coxiella burnetii, the Agent of Q Fever, in Murine Adipose Tissue. PLoS One. 2014;9:e97503.

490 6. Raoult D, Marrie T, Mege J. Natural history and pathophysiology of Q fever. The Lancet
491 Infectious Diseases. 2005;5:219-26.

492 7. van Schaik EJ, Chen C, Mertens K, Weber MM, Samuel JE. Molecular pathogenesis of the
493 obligate intracellular bacterium Coxiella burnetii. Nat Rev Microbiol. 2013;11:561-73.

494 8. Melenotte C, Protopopescu C, Million M, Edouard S, Carrieri MP, Eldin C, et al. Clinical
495 Features and Complications of Coxiella burnetii Infections From the French National Reference
496 Center for Q Fever. JAMA Netw Open. 2018;1:e181580.

497 9. Thuny F, Grisoli D, Cautela J, Riberi A, Raoult D, Habib G. Infective Endocarditis: Prevention,
498 Diagnosis, and Management. Canadian Journal of Cardiology. 2014;30:1046-57.

499 10. Martinez E, Cantet F, Fava L, Norville I, Bonazzi M. Identification of OmpA, a Coxiella
500 burnetii protein involved in host cell invasion, by multi-phenotypic high-content screening. PLoS

501 Pathog. 2014;10:e1004013.

502 11. Martinez E, Allombert J, Cantet F, Lakhani A, Yandrapalli N, Neyret A, et al. Coxiella burnetii
503 effector CvpB modulates phosphoinositide metabolism for optimal vacuole development. Proc
504 Natl Acad Sci U S A. 2016;113:E3260-3269.

505 12. Shipman M, Lubick K, Fouchard D, Gurram R, Grieco P, Jutila M, et al. Proteomic and Systems
506 Biology Analysis of the Monocyte Response to Coxiella burnetii Infection. Wang T, éditeur. PLoS
507 ONE. 2013;8:e69558.

508 13. Stead CM, Omsland A, Beare PA, Sandoz KM, Heinzen RA. Sec-mediated secretion by
509 Coxiella burnetii. BMC Microbiol. 2013;13:222.

510 14. Vodkin MH, Williams JC, Stephenson EH. Genetic Heterogeneity among Isolates of Coxiella
511 burnetii. Microbiology. 1986;132:455-63.

512 15. Hendrix LR, Samuel JE, Mallavia LP. Differentiation of Coxiella burnetii isolates by analysis
513 of restriction-endonuclease-digested DNA separated by SDS-PAGE. Microbiology.
514 1991;137:269-76.

515 16. Jäger C, Willems H, Thiele D, Baljer G. Molecular characterization of *Coxiella burnetii*
516 isolates. Epidemiol Infect. 1998;120:157-64.

517 17. Beare PA, Samuel JE, Howe D, Virtaneva K, Porcella SF, Heinzen RA. Genetic Diversity of
518 the Q Fever Agent, *Coxiella burnetii* , Assessed by Microarray-Based Whole-Genome
519 Comparisons. J Bacteriol. 2006;188:2309-24.

520 18. Hornstra HM, Priestley RA, Georgia SM, Kachur S, Birdsell DN, Hilsabeck R, et al. Rapid
521 Typing of Coxiella burnetii. Li W, éditeur. PLoS ONE. 2011;6:e26201.

522 19. Hoover TA, Culp DW, Vodkin MH, Williams JC, Thompson HA. Chromosomal DNA
523 Deletions Explain Phenotypic Characteristics of Two Antigenic Variants, Phase II and RSA 514
524 (Crazy), of the *Coxiella burnetii* Nine Mile Strain. Infect Immun. 2002;70:6726-33.

525 20. Toman R, Škultéty L. Structural study on a lipopolysaccharide from Coxiella burnetii strain
526 Nine Mile in avirulent phase II. Carbohydrate Research. 1996;283:175-85.
527 21. Q FEVER: REPORT OF A CASE SIMULATING LYMPHOMA. Ann Intern Med.
528 1957;47:1030.
529 22. Melenotte C, Million M, Audoly G, Gorse A, Dutronc H, Roland G, et al. B-cell non-Hodgkin
530 lymphoma linked to Coxiella burnetii. Blood. 2016;127:113-21.
531 23. van Roeden SE, van Houwelingen F, Donkers CMJ, Hogewoning SJ, de Lange MMA, van
532 der Hoek W, et al. Exposure to Coxiella burnetii and risk of non-Hodgkin lymphoma: a
533 retrospective population-based analysis in the Netherlands. The Lancet Haematology.
534 2018;5:e211-9.
535 24. Rothman N, Skibola CF, Wang SS, Morgan G, Lan Q, Smith MT, et al. Genetic variation in
536 TNF and IL10 and risk of non-Hodgkin lymphoma: a report from the InterLymph Consortium. The
537 Lancet Oncology. 2006;7:27-38.
538 25. Ghigo E, Capo C, Raoult D, Mege J-L. Interleukin-10 Stimulates *Coxiella burnetii* Replication
539 in Human Monocytes through Tumor Necrosis Factor Down-Modulation: Role in Microbicidal
540 Defect of Q Fever. Tuomanen EI, éditeur. Infect Immun. 2001;69:2345-52.
541 26. Melenotte C, Mezouar S, Ben Amara A, Benatti S, Chiaroni J, Devaux C, et al. A transcriptional
542 signature associated with non-Hodgkin lymphoma in the blood of patients with Q fever. Dolcetti
543 R, éditeur. PLoS ONE. 2019;14:e0217542.
544 27. Mezouar S, Omar Osman I, Melenotte C, Slimani C, Chartier C, Raoult D, et al. High
545 Concentrations of Serum Soluble E-Cadherin in Patients With Q Fever. Front Cell Infect
546 Microbiol. 2019;9:219.
547 28. van Roeden SE, van Houwelingen F, Donkers CMJ, Hogewoning SJ, de Lange MMA, van
548 der Hoek W, et al. Exposure to Coxiella burnetii and risk of non-Hodgkin lymphoma: a

549 retrospective population-based analysis in the Netherlands. Lancet Haematol. 2018;5:e211-9.
550 29. Weehuizen JM, van Roeden SE, Hogewoning SJ, van der Hoek W, Bonten MJM, Hoepelman
551 AIM, et al. No increased risk of mature B-cell non-Hodgkin lymphoma after Q fever detected:
552 results from a 16-year ecological analysis of the Dutch population incorporating the 2007-2010 Q
553 fever outbreak. Int J Epidemiol. 2022;dyac053.
554 30. Dash S, Duraivelan K, Samanta D. Cadherin-mediated host–pathogen interactions. Cellular
555 Microbiology [Internet]. 2021 [cité 18 mars 2022];23. Disponible sur:
556 https://onlinelibrary.wiley.com/doi/10.1111/cmi.13316
557 31. Ashton-Key M, Cowley GP, Smith ME. Cadherins in reactive lymph nodes and lymphomas:
558 high expression in anaplastic large cell lymphomas. Histopathology. 1996;28:55-9.
559 32. McCrea PD, Maher MT, Gottardi CJ. Nuclear Signaling from Cadherin Adhesion Complexes.
560 Current Topics in Developmental Biology [Internet]. Elsevier; 2015 [cité 23 mars 2022]. p. 129-96.
561 Disponible sur: https://linkinghub.elsevier.com/retrieve/pii/S0070215314000192
562 33. Vleminckx K, Vakaet L, Mareel M, Fiers W, Van Roy F. Genetic manipulation of E-cadherin
563 expression by epithelial tumor cells reveals an invasion suppressor role. Cell. 1991;66:107-19.
564 34. Christofori G, Semb H. The role of the cell-adhesion molecule E-cadherin as a tumour-
565 suppressor gene. Trends in Biochemical Sciences. 1999;24:73-6.
566 35. Pe N. Tumor suppressor gene E-cadherin and its role in normal and malignant cells. Cancer
567 Cell International. 2003;7.
568 36. Wells A, Yates C, Shepard CR. E-cadherin as an indicator of mesenchymal to epithelial
569 reverting transitions during the metastatic seeding of disseminated carcinomas. Clin Exp
570 Metastasis. 2008;25:621-8.
571 37. Izaguirre MF, Galetto CD, Baró L, Casco VH. E-Cadherin Dysfunction and Cancer. Journal of
572 Biosciences and Medicines. Scientific Research Publishing; 2019;7:42-67.

573 38. Na T-Y, Schecterson L, Mendonsa AM, Gumbiner BM. The functional activity of E-cadherin
574 controls tumor cell metastasis at multiple steps. Proc Natl Acad Sci USA. 2020;117:5931-7.
575 39. Grabowska MM, Day ML. Soluble E-cadherin: More Than a Symptom of Disease. Front Biosci
576 (Landmark Ed). 2012;17:1948-64.
577 40. Devaux CA, Mezouar S, Mege J-L. The E-Cadherin Cleavage Associated to Pathogenic
578 Bacteria Infections Can Favor Bacterial Invasion and Transmigration, Dysregulation of the
579 Immune Response and Cancer Induction in Humans. Front Microbiol. 2019;10:2598.
580 41. Aghababaei M, Hogg K, Perdu S, Robinson WP, Beristain AG. ADAM12-directed ectodomain
581 shedding of E-cadherin potentiates trophoblast fusion. Cell Death Differ. 2015;22:1970-84.
582 42. Capo C, Lindberg FP, Meconi S, Zaffran Y, Tardei G, Brown EJ, et al. Subversion of monocyte
583 functions by coxiella burnetii: impairment of the cross-talk between alphavbeta3 integrin and CR3.
584 J Immunol. 1999;163:6078-85.
585 43. Ghigo E, Imbert G, Capo C, Raoult D, Mege J-L. Interleukin-4 Induces *Coxiella burnetii*
586 Replication in Human Monocytes but not in Macrophages. Annals of the New York Academy of
587 Sciences. 2003;990:450-9.
588 44. Heystek HC, Mudde GC, Ohler R, Kalthoff FS. Granulocyte-macrophage colony-stimulating
589 factor (GM-CSF) has opposing effects on the capacity of monocytes versus monocyte-derived
590 dendritic cells to stimulate the antigen-specific proliferation of a human T cell clone. Clin Exp
591 Immunol. 2000;120:440-7.
592 45. Saito H, Kato A, Matsumoto K, Okayama Y. Culture of human mast cells from peripheral
593 blood progenitors. Nat Protoc. 2006;1:2178-83.
594 46. Winer J, Jung CKS, Shackel I, Williams PM. Development and Validation of Real-Time
595 Quantitative Reverse Transcriptase–Polymerase Chain Reaction for Monitoring Gene Expression
596 in Cardiac Myocytesin Vitro. Analytical Biochemistry. 1999;270:41-9.

597 47. Shannon JG, Heinzen RA. Adaptive immunity to the obligate intracellular pathogen Coxiella
598 burnetii. Immunol Res. 2009;43:138-48.
599 48. Sireci G, Badami GD, Di Liberto D, Blanda V, Grippi F, Di Paola L, et al. Recent Advances
600 on the Innate Immune Response to Coxiella burnetii. Front Cell Infect Microbiol. 2021;11:754455.
601 49. Zarza SM, Mezouar S, Mege J-L. From Coxiella burnetii Infection to Pregnancy
602 Complications: Key Role of the Immune Response of Placental Cells. Pathogens. 2021;10:627.
603 50. Graham JG, Winchell CG, Kurten RC, Voth DE. Development of an *Ex Vivo* Tissue Platform
604 To Study the Human Lung Response to Coxiella burnetii. Roy CR, éditeur. Infect Immun.
605 2016;84:1438-45.
606 51. Dragan AL, Kurten RC, Voth DE. Characterization of Early Stages of Human Alveolar
607 Infection by the Q Fever Agent *Coxiella burnetii*. Roy CR, éditeur. Infect Immun. 2019;87:e00028-
608 19.
609 52. Coutifaris C, Kao LC, Sehdev HM, Chin U, Babalola GO, Blaschuk OW, et al. E-cadherin
610 expression during the differentiation of human trophoblasts. Development. 1991;113:767-77.
611 53. Lecuit M, Nelson DM, Smith SD, Khun H, Huerre M, Vacher-Lavenu M-C, et al. Targeting
612 and crossing of the human maternofetal barrier by *Listeria monocytogenes* : Role of internalin
613 interaction with trophoblast E-cadherin. Proc Natl Acad Sci USA. 2004;101:6152-7.
614 54. Coleman SA, Fischer ER, Howe D, Mead DJ, Heinzen RA. Temporal Analysis of *Coxiella*
615 *burnetii* Morphological Differentiation. J Bacteriol. 2004;186:7344-52.
616 55. Meconi S, Capo C, Remacle-Bonnet M, Pommier G, Raoult D, Mege J-L. Activation of Protein
617 Tyrosine Kinases by Coxiella burnetii: Role in Actin Cytoskeleton Reorganization and Bacterial
618 Phagocytosis. Infect Immun. 2001;69:2520-6.
619 56. Voth DE, Heinzen RA. Sustained Activation of Akt and Erk1/2 Is Required for *Coxiella*
620 *burnetii* Antiapoptotic Activity. Infect Immun. 2009;77:205-13.

621 57. Zheng G, Lyons JG, Tan TK, Wang Y, Hsu T-T, Min D, et al. Disruption of E-Cadherin by
622 Matrix Metalloproteinase Directly Mediates Epithelial-Mesenchymal Transition Downstream of
623 Transforming Growth Factor-β1 in Renal Tubular Epithelial Cells. The American Journal of
624 Pathology. 2009;175:580-91.
625 58. Marambaud P. A presenilin-1/gamma-secretase cleavage releases the E-cadherin intracellular
626 domain and regulates disassembly of adherens junctions. The EMBO Journal. 2002;21:1948-56.
627 59. Kourtidis A, Ngok SP, Anastasiadis PZ. p120 Catenin. Progress in Molecular Biology and
628 Translational Science [Internet]. Elsevier; 2013 [cité 23 mars 2022]. p. 409-32. Disponible sur:
629 https://linkinghub.elsevier.com/retrieve/pii/B9780123943118000182
630 60. O'Connor PM, Lapointe TK, Jackson S, Beck PL, Jones NL, Buret AG. Helicobacter pylori
631 Activates Calpain via Toll-Like Receptor 2 To Disrupt Adherens Junctions in Human Gastric
632 Epithelial Cells. Blanke SR, éditeur. Infect Immun. 2011;79:3887-94.
633 61. Wu S, Morin PJ, Maouyo D, Sears CL. Bacteroides fragilis enterotoxin induces c-Myc
634 expression and cellular proliferation. Gastroenterology. 2003;124:392-400.
635 62. Chung L, Thiele Orberg E, Geis AL, Chan JL, Fu K, DeStefano Shields CE, et al. Bacteroides
636 fragilis Toxin Coordinates a Pro-carcinogenic Inflammatory Cascade via Targeting of Colonic
637 Epithelial Cells. Cell Host & Microbe. 2018;23:203-214.e5.
638 63. Meconi S, Jacomo V, Boquet P, Raoult D, Mege J-L, Capo C. Coxiella burnetii Induces
639 Reorganization of the Actin Cytoskeleton in Human Monocytes. Infect Immun. 1998;66:5527-33.
640 64. Ayollo DV, Zhitnyak IY, Vasiliev JM, Gloushankova NA. Rearrangements of the Actin
641 Cytoskeleton and E-Cadherin–Based Adherens Junctions Caused by Neoplasic Transformation
642 Change Cell–Cell Interactions. Hartl D, éditeur. PLoS ONE. 2009;4:e8027.
643 65. Khan NI, Bradstock KF, Bendall LJ. Activation of Wnt/?-catenin pathway mediates growth
644 and survival in B-cell progenitor acute lymphoblastic leukaemia. Br J Haematol. 2007;138:338-48.

645 66. Mani M, Carrasco DE, Zhang Y, Takada K, Gatt ME, Dutta-Simmons J, et al. BCL9 Promotes
646 Tumor Progression by Conferring Enhanced Proliferative, Metastatic, and Angiogenic Properties
647 to Cancer Cells. Cancer Res. 2009;69:7577-86.

648

649

650

651

652

653

654

655

656

657

658

659

660

661

662

663

664

665

666

667

668

669 **Table 1. Specific primers used for q-RTPCR assays**

670

Genes (symbols)	Primers sequence	
	Sense	Antisense
Adenomatous polyposis coli (*APC*)	AGC-ACT-CCA-CCA-CAT-CAT-TCA-C	TTA-GAA-CAC-ACA-CAG-CAG-GAC-A
β-catenin (*CTNNB1*)	TCC-CTT-GGC-TGA-GTA-TTT-CTT-C	CAC-TGC-CTC-TTT-CCT-TAC-ATC-C
B-cell CLL/lymphoma 9 protein (*BCL9*)	TGT-TTT-CTA-CCC-CAG-GAC-TCT-C	CTA-TCG-TCT-CTT-TCC-ACA-TCC-A
Cyclin-dependent kinase 1 (*CCND1*)	ATC-CAG-TGA-CAA-ACC-ATC-CAG-T	TTG-GGT-AGA-AAA-CCA-GCA-TCT-C
E-cadherin (*CDH1*)	GAA-GGT-GAC-AGA-GCC-TCT-GGA-T	GAT-CGG-TTA-CCG-TGA-TCA-AAA-T
Frizzled Class receptor 1 (*FZD1*)	CCC-TCC-TAC-CTC-AAC-TAC-CAC-TT	ATT-ACA-CAC-CAC-TCG-GTC-TTC-C
Naked cuticle 2 (NC2)	GCC-TTA-GAG-CCA-GGA-AAC-ATA-G	CGA-CAG-CAA-ACA-GCA-ACT-GAC
Transcription factor 7-like 2 (*TCF7L2*)	GCT-ACG-ACC-TTT-GCT-CTC-ATT-T	ATC-ACG-ACA-GGA-GGA-TTC-AGA-C
Wnt Family Member 3A (*WNT3A*)	TGA-GAC-GGGG-CTC-CTT-CGG-CA	TGG-AGC-CGG-GAT-TCT-TGCAGG-T
Wnt Family Member 5A (*WNT5A*)	CAG-CAT-TCC-ACA-AAC-ACT-T	TTC-ACC-ATT-CCA-CAG-AGA-GAG-A
Wnt Family Member 9B (*WNT9B*)	GGA-AAA-TAC-CAC-AAC-CCC-ACC-T	GAC-CAC-TGA-CCC-CTC-ATT-CTA-C

671

672

673

674 # Figures and legends

675 **Fig 1. Selection of a cellular *in vitro* model to study E-cad modulation.**

676 **(A)** Immunoblot detection of E-cad expression in protein lysates of various cell types including
677 HeLa, THP-1, MRC-5, and the BeWo cell line and primary human monocytes **(B)** Cellular
678 localization/distribution of E-cad protein (red), actin (green) and nucleus (blue) in three different
679 cell types (BeWo cells, MRC-5 cells, monocytes). Images were acquired using a confocal
680 microscope (Zeiss LSM 800) with a 63X/1.4 oil objective (Scale bar: 10 µm). (**C**) Scanning
681 electron microscopy images of the ultra-thin section of BeWo cells infected with virulent *Coxiella*
682 *burnetii* Nine Mile (**a**) or *Coxiella burnetii* Guiana strain (**c**). **(b)** and (**d**) respectively high
683 magnification of the boxed region in **(a)** and **(c)** show a vacuole-contained *Coxiella burnetii*-like
684 bacteria (white arrows).

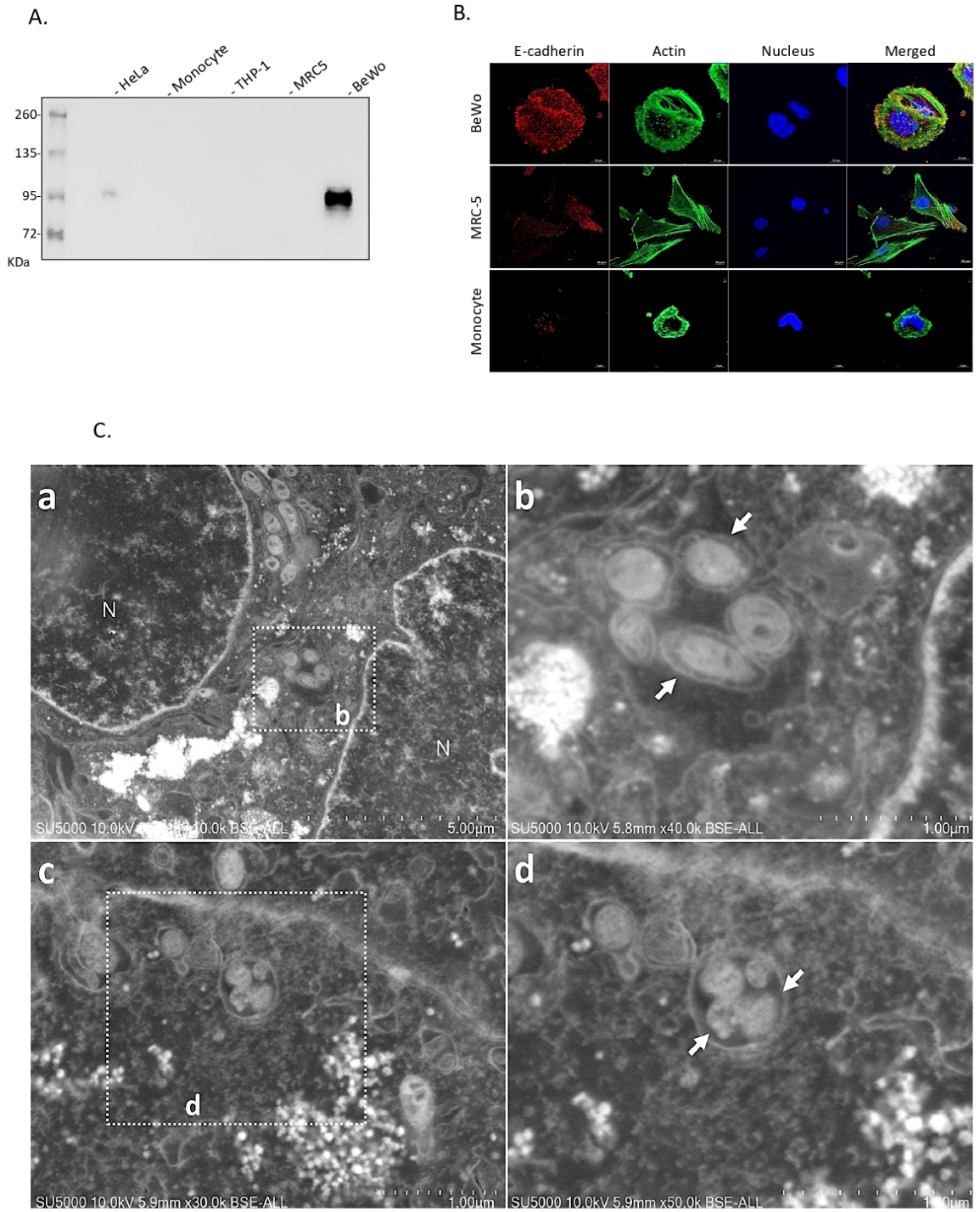
A.
HeLa
Monocyte
THP-1
MRC5
BeWo
260-
135-
95-
72-
KDa
B.
E-cadherin
Actin
Nucleus
Merged
BeWo
MRC-5
Monocyte
C.
a
N
b
N
SU5000 10.0kV 5.8mm x40.0k BSE-ALL
5.00µm
b
SU5000 10.0kV 5.8mm x40.0k BSE-ALL
1.00µm
c
d
SU5000 10.0kV 5.9mm x30.0k BSE-ALL
1.00µm
d
SU5000 10.0kV 5.9mm x50.0k BSE-ALL

685

686

687

688 **Fig 2. Modulation of E-cad expression in BeWo cells either exposed to live *C. burnetii* or *E.***
689 ***coli* LPS**.

690 (**A)** Flow cytometry analysis of E-cad expression at the surface of BeWo cells. Cells were incubated
691 with live *C. burnetii* Nine Mile strain or were stimulated with *E. coli* LPS for 24 hours (n = 3).
692 BeWo cells maintained in cultured medium without additive (unstimulated) were used as control.
693 The two panels show the gating parameter chosen and the quantification of E-cad, respectively.
694 **(B)** Histogram indicating the percent of cells expressing E-cad. **(C)** Histogram representing the
695 mean fluorescence intensity (MFI) under the different experimental conditions. The non-
696 parametric Mann-Whitney test was used for statistical analysis of all data. The p value < 0.05:
697 symbol *; p value <0.01: symbol **. **(D)** The panel presents *C. burnetii* (live or heat-inactivated
698 bacterium) exposed cells versus *E. coli* LPS stimulated cells and evaluation of fluorescence
699 corresponding to the E-cad (red), *C. burnetii* (white), actin (green), and the nucleus of the cells
700 (blue). Images were acquired using a confocal microscope (Zeiss LSM 800) with a 63X/1.4 oil
701 objective (scale bar: 20 µm).

A.

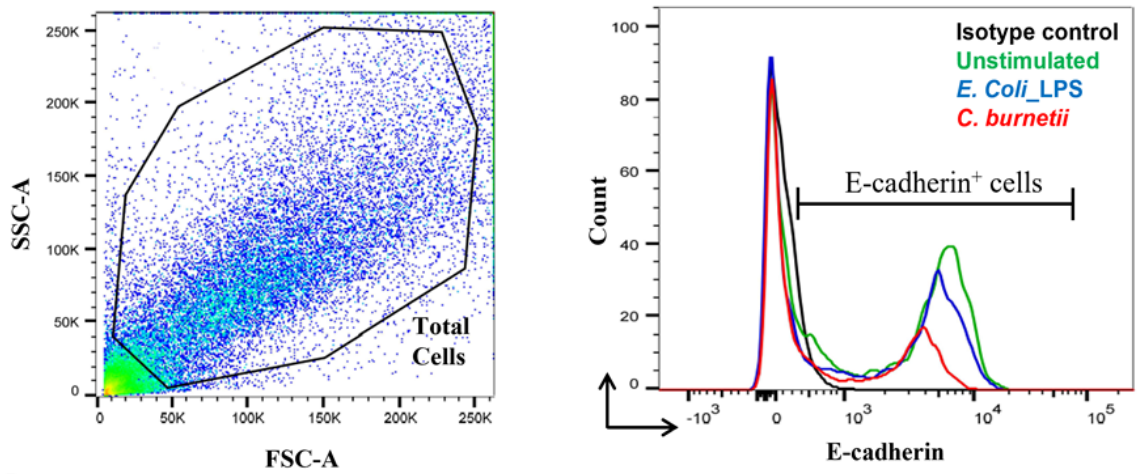
SSC-A
FSC-A
Total Cells
Isotype control
Unstimulated
E. Coli_LPS
C. burnetii
E-cadherin+ cells
Count
E-cadherin

B.

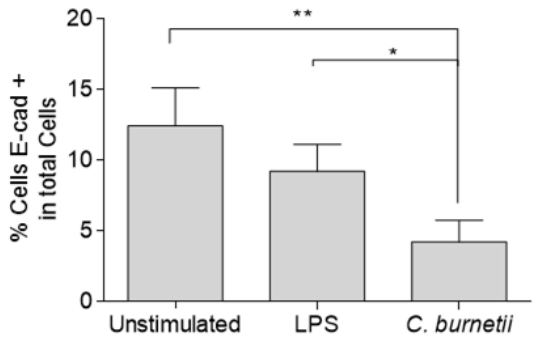
% Cells E-cad + in total Cells
Unstimulated
LPS
C. burnetii

C.

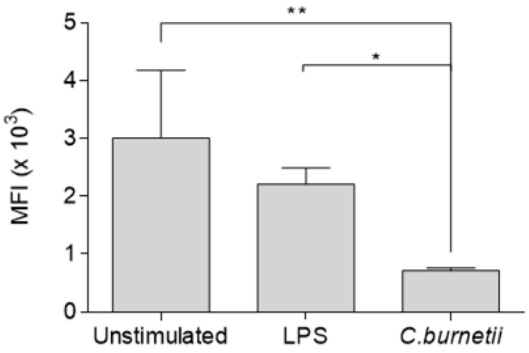
MFI (x 10^3)
Unstimulated
LPS
C.burnetii

D.

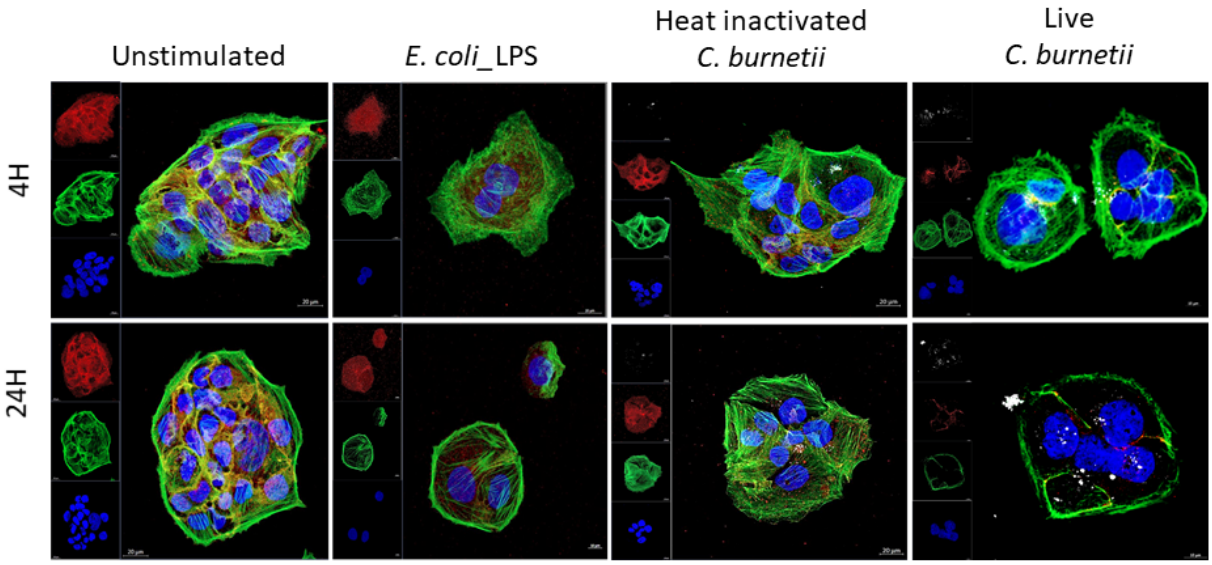
Unstimulated
E. coli_LPS
Heat inactivated C. burnetii
Live C. burnetii
4H
24H

702

703

704 **Fig 3. Impact of *C. burnetii* infection of BeWo cells on their E-cad expression**.

705 BeWo cells were incubated with live *Coxiella burnetii* Nine Mile strain for 4, 8, 24, and 48 hours
706 (n=3)**. (A)** ELISA quantification of sE-cad released in the supernatant of BeWo cells under
707 different experimental conditions (unstimulated, *E. coli* LPS-stimulated, *C. burnetii* Nine Mile
708 strain-infected), at different times of experiment. **(B)** qRT-PCR analysis of *CDH1*/E-cadherin and
709 *CTNNB1*/β-catenin mRNAs expression in BeWo cells exposed *in vitro* during 48 hours to *C.*
710 *burnetii* Nine Mile strain or the *E. coli* LPS. Expression level of investigated genes was illustrated
711 as ± SEM of the fold change ($FC = 2^{-\Delta\Delta Ct}$, where $\Delta\Delta Ct = [(Ct_{target} - Ct_{actin})$ stimulated$] - [(Ct_{target} -$
712 $Ct_{actin})$ unstimulated] and p values was evaluated according to an ordinary Two-way Anova test).
713 **(C)** Blots were spliced after protein transfer and then were probed with antibodies. Upper panel:
714 Immunoblot detection of E-cad (upper blot), β-catenin (middle blot) and β-actin (lower blot)
715 expression in total protein lysates of BeWo cells cultured under the three different experimental
716 conditions described above (unstimulated, LPS-stimulated, *C. burnetii*-infected), at 8 and 24 hours
717 post treatment. The histogram shown in the lower panel is a quantification of E-cad and β-catenin
718 expression with respect to β-actin. The p value < 0.05: symbol *; p value <0.01: symbol **
719

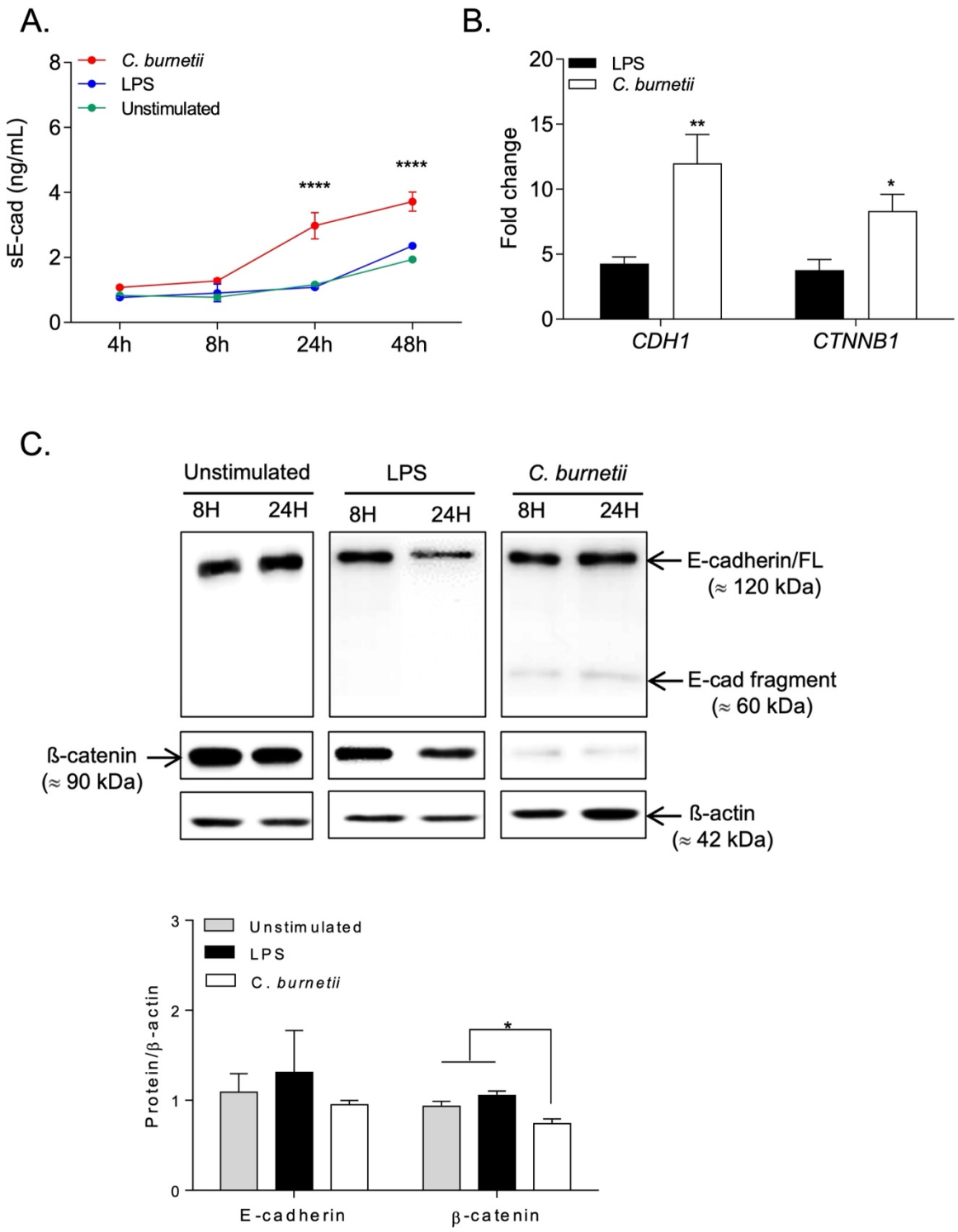
A.
C. burnetii
LPS
Unstimulated
sE-cad (ng/mL)
8
6
4
2
0
****
****
4h
8h
24h
48h
B.
LPS
C. burnetii
Fold change
20
15
10
5
0
**
*
CDH1
CTNNB1
C.
Unstimulated
LPS
C. burnetii
8H
24H
8H
24H
8H
24H
E-cadherin/FL
(≈ 120 kDa)
E-cad fragment
(≈ 60 kDa)
ß-catenin
(≈ 90 kDa)
ß-actin
(≈ 42 kDa)
Unstimulated
LPS
C. burnetii
Protein/β-actin
3
2
1
0
*
E-cadherin
β-catenin

720

721

722 **Fig 4**. **Impact of *C. burnetii* (Nine Mile strain or Guiana strain) infection of BeWo cells on the**
723 **expression of *CDH1*/E-cad, *CTNNB1*/β-catenin and other genes involved in the**
724 **Wnt/frizzled/β-catenin pathways.**

725 BeWo cells were exposed in *vitro* for 48 h to *C. burnetii* Nine Mile strain or Guiana (Cb 175) strain
726 (live and heat-inactivated strain) or were stimulated with *E. coli* LPS. The expression (n=6) of
727 *CDH1*/E-cad **(A)**, *CTNNB1*/β-catenin **(B)** and other genes involved in the Wnt/frizzled/β-catenin
728 pathways **(C to K)**, was investigated by qRT-PCR after normalization with the housekeeping actin
729 gene as endogenous control. Expression level of investigated genes was illustrated as ± SEM of
730 the fold change ($FC = 2^{-\Delta\Delta Ct}$, where $\Delta\Delta Ct = [(Ct_{target} - Ct_{actin})$ stimulated$] - [(Ct_{target} - Ct_{actin})$
731 unstimulated] and compared using the Kruskal-Wallis test. The p value < 0.05: symbol *; p value
732 <0.01: symbol **; p value < 0.001: symbol ***; p value <0.0001: symbol ****

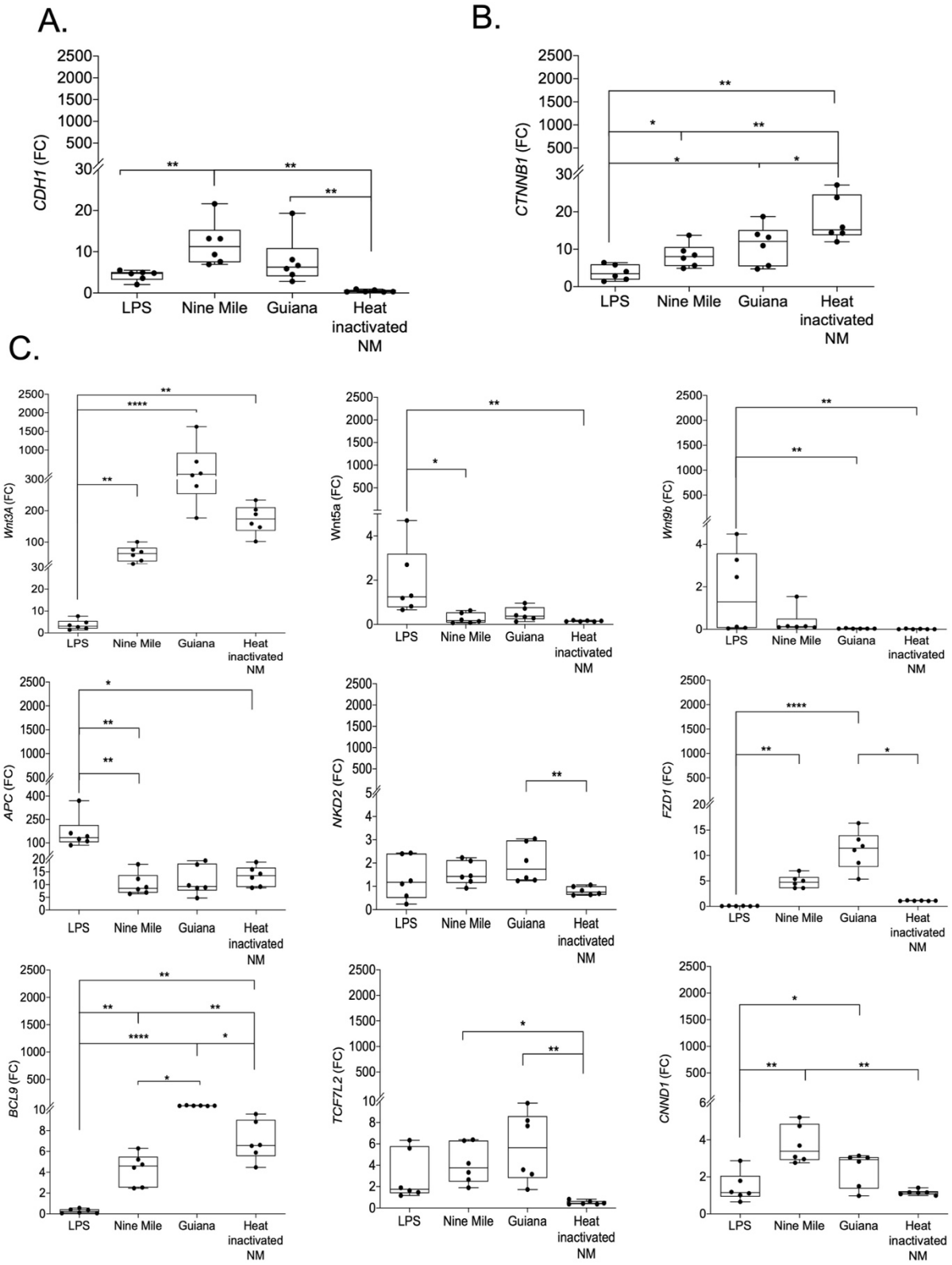
A.
CDH1 (FC)
LPS
Nine Mile
Guiana
Heat inactivated NM
B.
CTNNB1 (FC)
C.
Wnt3A (FC)
Wnt5a (FC)
Wnt9b (FC)
APC (FC)
NKD2 (FC)
FZD1 (FC)
BCL9 (FC)
TCF7L2 (FC)
CNND1 (FC)

733

734 **Fig 5. Principal component analysis and hierarchical clustering. BeWo cells were infected or**
735 **not with different strains of *C. burnetii* (live or heat inactivated) for 48 h**.
736 The transcripts of several genes were quantified by qRT-PCR. Results (n=6) were expressed as RE
737 $= 2^{-\Delta CT}$, where $\Delta ct = (Ct_{target} - Ct_{actin})$. Principal component analysis **(A)** and hierarchical clustering
738 **(B)** were performed to show the distribution of the different groups of infected/stimulated BeWo
739 cells and the modulation of expression of different genes, including *CDH1*/E-cad, *CTNNB1*/β-
740 catenin and other genes involved in the Wnt/frizzled/β-catenin pathways, such as WNT3A,
741 WNT5A, WNT9B.

A.

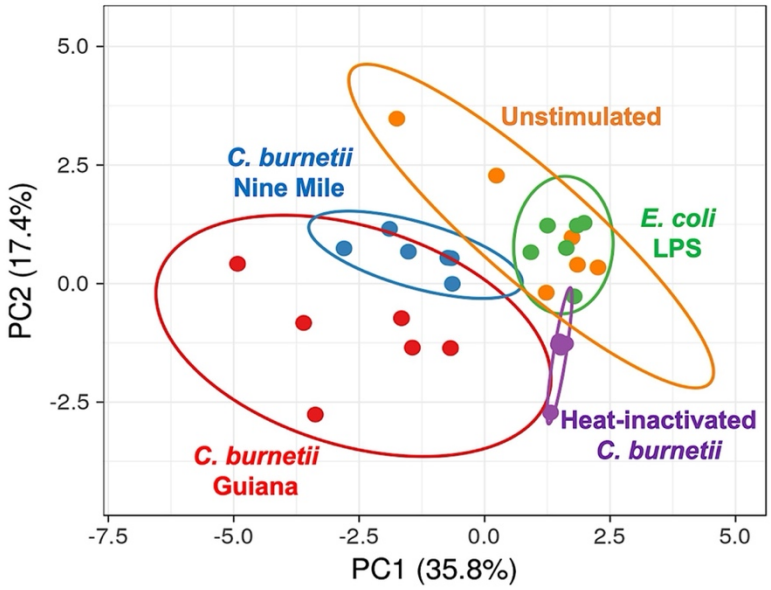
Unstimulated
C. burnetii
Nine Mile
E. coli
LPS
Heat-inactivated
C. burnetii
C. burnetii
Guiana
PC2 (17.4%)
PC1 (35.8%)
5.0
2.5
0.0
-2.5
-7.5
-5.0
-2.5
0.0
2.5
5.0

B.

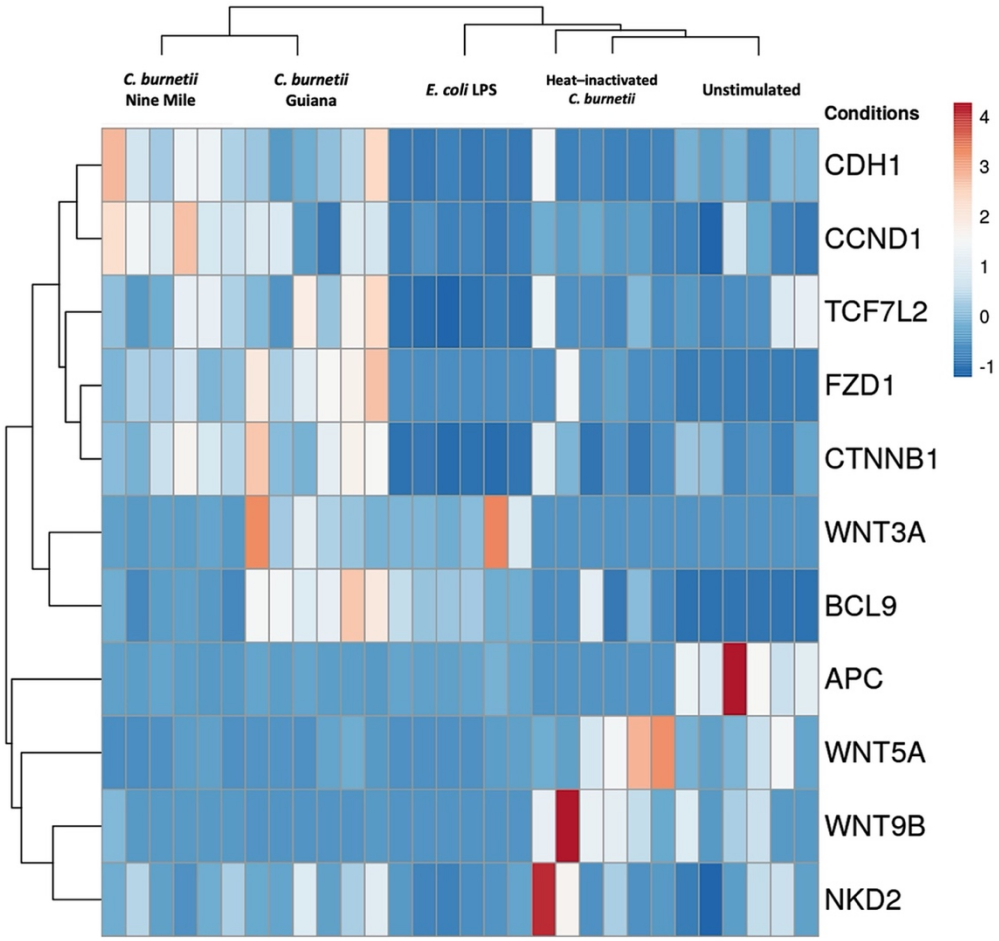
C. burnetii
Nine Mile
C. burnetii
Guiana
E. coli LPS
Heat–inactivated
C. burnetii
Unstimulated
Conditions
CDH1
CCND1
TCF7L2
FZD1
CTNNB1
WNT3A
BCL9
APC
WNT5A
WNT9B
NKD2
4
3
2
1
0
-1

742

743 **Supporting Information**

744 **S1 Fig. Scanning electron microscopy images of the ultra-thin section of a trophoblast cell**
745 **incubated with *Coxiella* bacteria. (A, B, C)** SEM images of *C. burnetii* Guiana strain infected
746 BeWo cells. **(B)** High magnification of the boxed region in **(A)** shows serval vacuoles dispersed in
747 the cell cytoplasm. **(C)** High magnification of the boxed region in **(B)** shows a vacuole containing
748 electron-dense circular structures resembling *C. burnetii* (white arrows). **(D, E, F)** SEM images of
749 *C. burnetii* Nine Mile strain infected BeWo cells. **(D)** High magnification of the boxed region in
750 **(E)** shows vacuoles inside the BeWo cell **(F)** filled with hypo electron-dense *C. burnetii*-like
751 structures with or without less electron-dense internal content (white arrows).

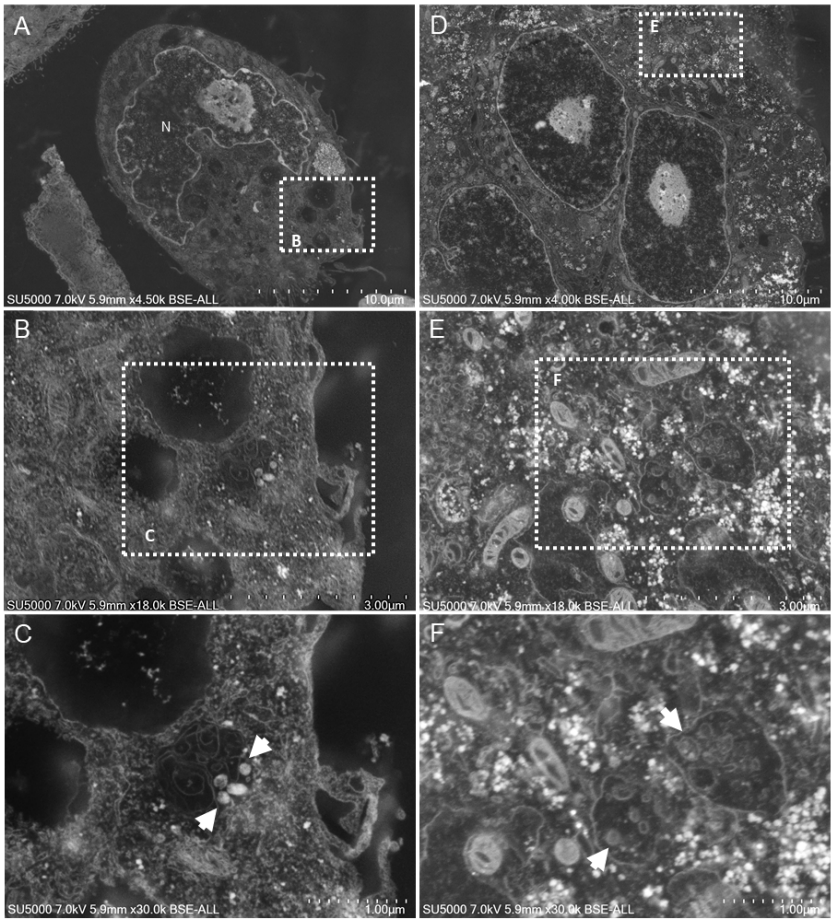

752

753 **S2 Fig. Confocal microscopy analysis of BeWo cells at 5 min post-infection with *C. burnetii*.**
754 Fluorescence labelling was as follows: *C. burnetii* (white), E-cad (red), actin (green), and cell
755 nucleus (blue). Images were acquired using a confocal microscope (Zeiss LSM 800) with a 63X/1.4
756 oil objective (scale bar: 20 µm). Regions of high concentration of *C. burnetii* are shown with higher
757 magnitude within scales.

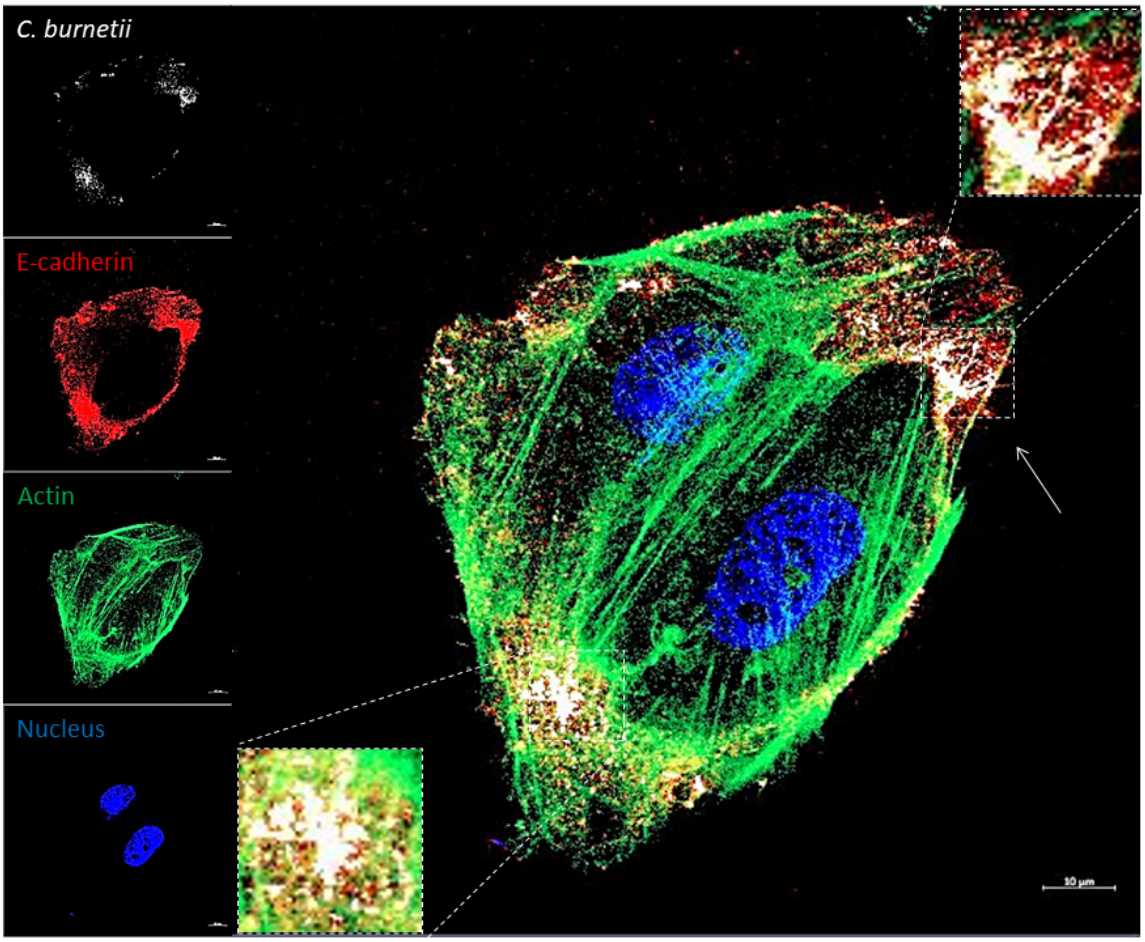

758
759
760
761
762
763

764 **S3 Fig. Confocal microscopy analysis of BeWo cells at 4 hours post-infection with *C. burnetii***
765 **(Cb) Guiana strain.** Fluorescence labelling was as follows: *C. burnetii* (white), E-cad (red), actin
766 (green), and cell nucleus (blue). Images were acquired using a confocal microscope (Zeiss LSM
767 800) with a 63X/1.4 oil objective (scale bar: 20 µm).
768

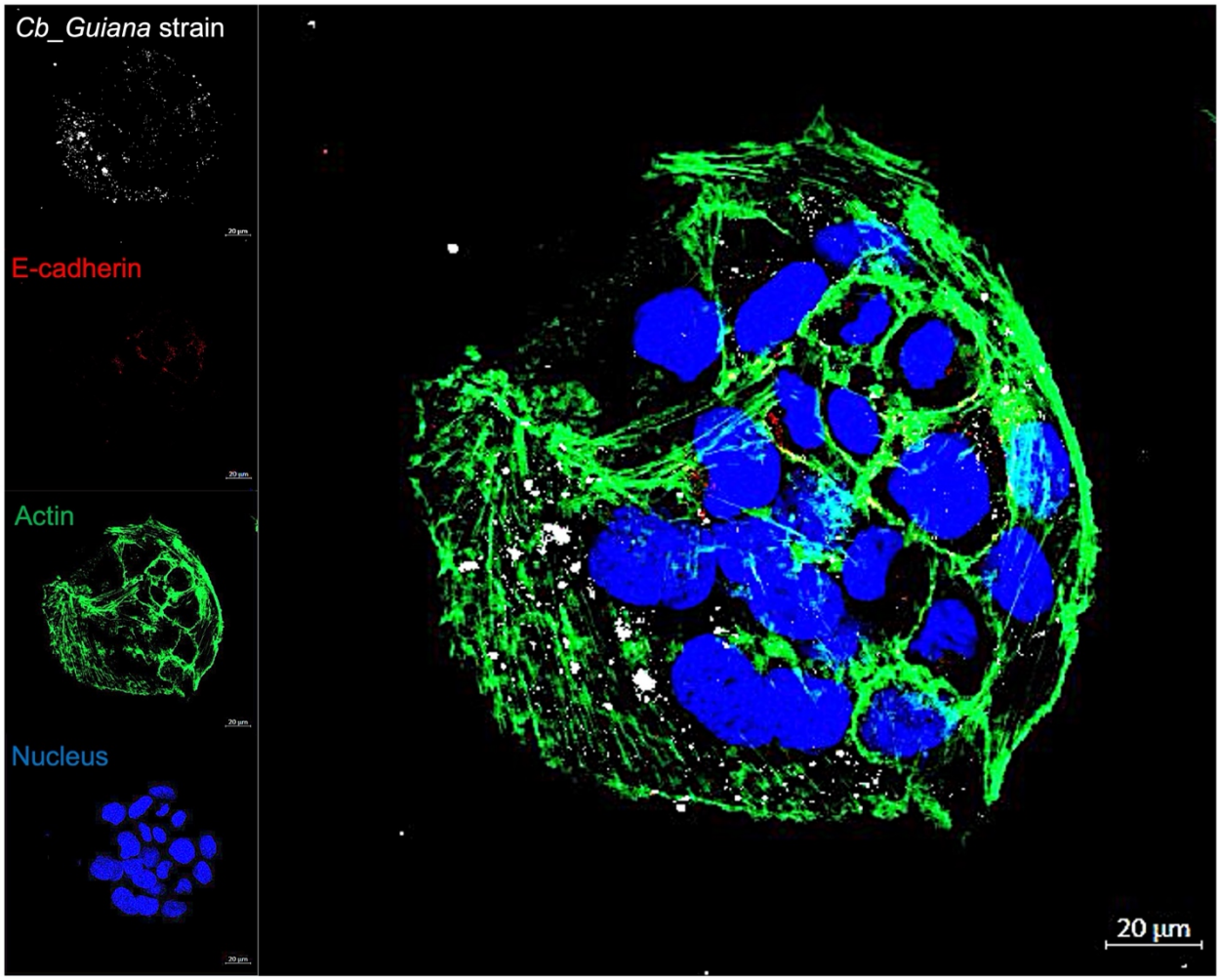

769
770
771
772

773 **S4 Fig. Exploration of gene signatures of *C. burnetii* infection (Nine Mile laboratory strain)**
774 **of human cells as evidenced by microarray analysis.** BeWo cells infected or not by *C. burnetii*
775 were submitted to microarray analysis as well as primary cells, including monocyte-derived
776 macrophages (MDM), monocyte-derived dendritic cells (moDC), and mast cells. **(A)** Set of genes
777 up- or down-modulated in the panel of *C. burnetii* infected cells compared to uninfected cells (e.g.,
778 6942 genes up-regulated and 12199 genes down-regulated in BeWo cells after *C. burnetii*
779 infection). **(B)** principal component analysis and **(C)** hierarchical clustering were performed to
780 show the distribution of the different groups of infected cells and the modulation of gene
781 expression.
782
783

A.

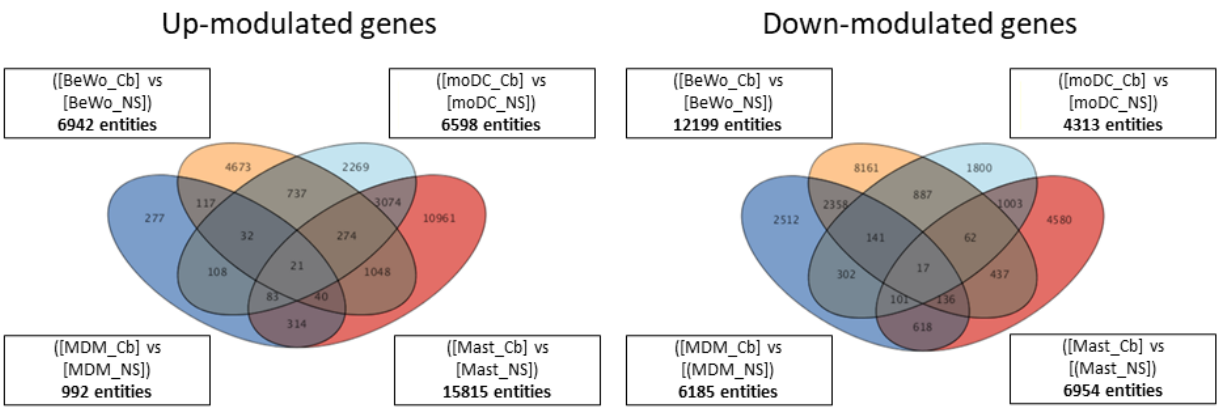
Up-modulated genes
([BeWo_Cb] vs [BeWo_NS]) 6942 entities
([moDC_Cb] vs [moDC_NS]) 6598 entities
([MDM_Cb] vs [MDM_NS]) 992 entities
([Mast_Cb] vs [Mast_NS]) 15815 entities
4673
2269
737
117
3074
277
10961
32
274
108
21
1048
83
40
314
Down-modulated genes
([BeWo_Cb] vs [BeWo_NS]) 12199 entities
([moDC_Cb] vs [moDC_NS]) 4313 entities
([MDM_Cb] vs [(MDM_NS]) 6185 entities
([Mast_Cb] vs [(Mast_NS]) 6954 entities
8161
1800
887
2358
1003
2512
4580
141
62
302
17
437
101
136
618

B.

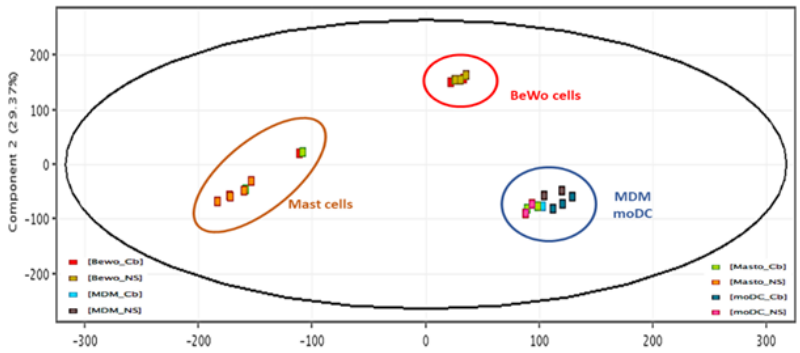
Component 2 (29.37%)
BeWo cells
Mast cells
MDM
moDC
[Bewo_Cb]
[Bewo_NS]
[MDM_Cb]
[MDM_NS]
[Masto_Cb]
[Masto_NS]
[moDC_Cb]
[moDC_NS]
200
100
0
-100
-200
-300
-200
-100
0
100
200
300

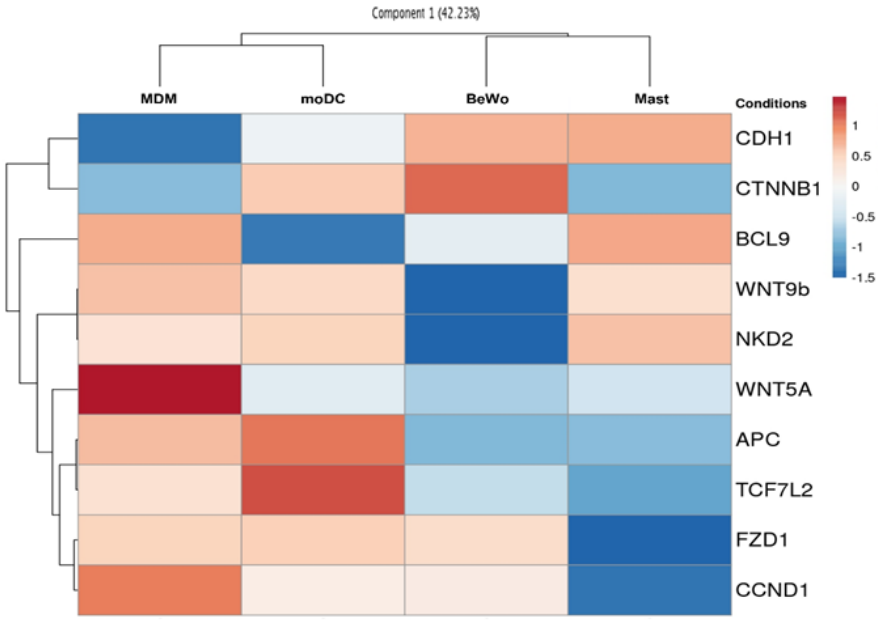
Component 1 (42.23%)
MDM
moDC
BeWo
Mast
Conditions
CDH1
CTNNB1
BCL9
WNT9b
NKD2
WNT5A
APC
TCF7L2
FZD1
CCND1
1
0.5
0
-0.5
-1
-1.5

784

785